frontiers | Frontiers in Materials

TYPE Original Research
PUBLISHED 07 September 2022
DOI 10.3389/fmats.2022.966692

OPEN ACCESS

EDITED BY
Shanker Govindaswamy,
Bangalore University, India

REVIEWED BY
Gurumurthy Hegde,
Christ University, India
Hale Ocak,
Yıldız Technical University, Turkey

*CORRESPONDENCE
Kiwoong Kim,
kwkim@hnu.kr

SPECIALTY SECTION
This article was submitted to Polymeric and Composite Materials, a section of the journal Frontiers in Materials

RECEIVED 20 June 2022
ACCEPTED 15 August 2022
PUBLISHED 07 September 2022

CITATION
Shi Y and Kim K (2022), Fabrication of hydrophilic and hydrophobic membranes inspired by the phenomenon of water absorption and storage of cactus.
Front. Mater. 9:966692.
doi: 10.3389/fmats.2022.966692

Fabrication of hydrophilic and hydrophobic membranes inspired by the phenomenon of water absorption and storage of cactus

Yana Shi and Kiwoong Kim*

Department of Mechanical Engineering, Hannam University, Daejeon, South Korea

Water shortage has become one of the most severe practical problems facing humans. Thus, an efficient and economic water-harvesting technology is urgent to develop. In this work, to prepare samples of hydrophilic and hydrophobic bilayer structures, three kinds of hydrophobic polyethylene terephthalate (PET) fibers with different pore diameters were dip coated to fabricate hydrophobic surfaces, which showed different hydrophobic effects. TiO_2 was then sprayed onto the hydrophobic surface to form irregular protrusions and to increase surface roughness and surface energy. The distribution amount of TiO_2 was controlled by adjusting the spraying distance of TiO_2. Finally, ultraviolet irradiation was performed. The light response made the protrusions super hydrophilic and improved the capture of mist and moisture by increasing the surface wettability and Laplace pressure. Water-collection test was performed for samples with different spraying distances irradiated by ultraviolet rays. The spraying distance with the best water-collection efficiency was achieved. The hydrophilic surface (particles) was attached to a hydrophobic membrane, which quickly and effectively captured the mist and converted it to water, thereby easily discharging a large amount of water. This study is expected to promote the development of fogging drainage and alleviate the problem of water shortage.

KEYWORDS

water shortage, spray coating method, light response, hydrophilic, hydrophobic

1 Introduction

The Global Water Scarcity Assessment measures water scarcity every year. Water scarcity has become a serious global and local problem, posing a threat to human health, economic growth, and living standards. Freshwater scarcity is seen as a global systemic risk (Postel et al., 1996; Vorosmarty et al., 2000; Van Der Vegt et al., 2015; Mekonnen and Hoekstra, 2016).

To solve the problem of water shortage, water harvesting is the core technology for collecting fresh water in arid regions (Lee et al., 2019). Nature with its long-term evolution

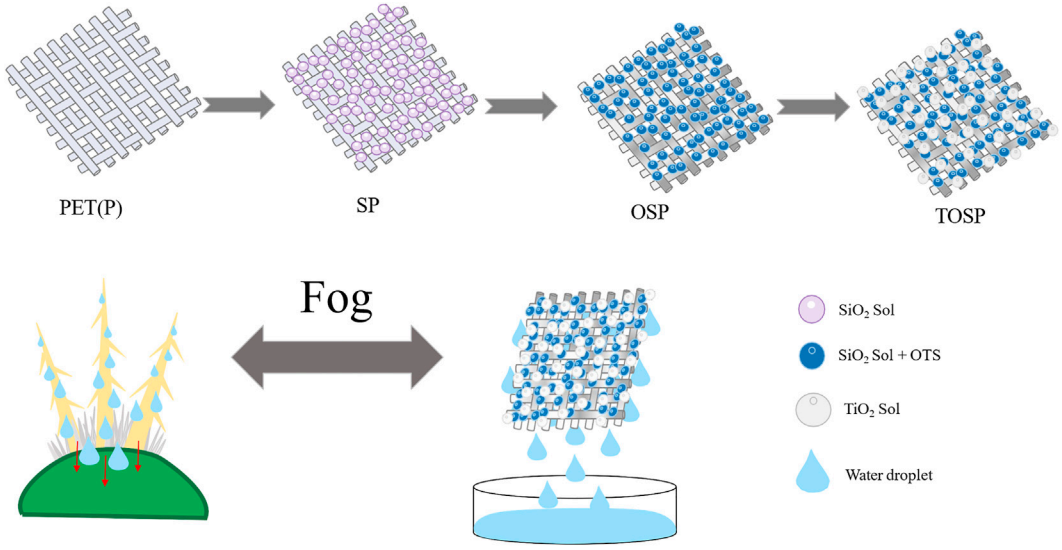

FIGURE 1
The Preparation process of hydrophilic–hydrophobic double-layer structure sample and water-collection and drainage phenomenon. Based on polyethylene terephthalate (PET), P was initially dipped with SiO_2 and hydrophilic SP was obtained after drying. Then, OTS was dipped into SP, SP was chemically modified, and hydrophobic OSP was obtained after drying. Finally, OSP was sprayed with TiO_2, followed by UV light response to obtain hydrophilic–hydrophobic double-layer structure TOSP. The water collecting and drainage mechanism of cacti to fog and the water collecting and drainage phenomenon of the sample with double structure prepared to fog. Representation of important elements in the diagram. The blue ball represents SiO_2 particles after dipping and drying; The purple sphere represents the chemically modified particles of SiO_2 soaked in OTS. White spheres represent spray TiO_2 particles, and sky blue droplets represent water droplets.

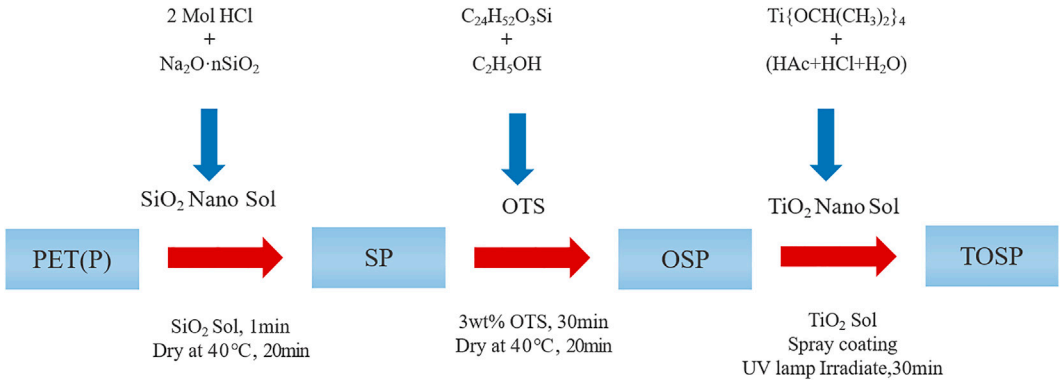

FIGURE 2
Sample processing.

and natural selection is the best museum in the world, providing humans with many bionic inspirations (Xue and Jiang, 2012; Liu et al., 2017). Some organisms such as the Namib desert beetle (Parker and Lawrence, 2001), spider silk (Zheng et al., 2010), and cactus clusters (Ju et al., 2012) feature interesting water-harvesting ability, thereby attracting extensive research attention in the field of water harvesting and bionic research.

Atmospheric water is equivalent to about 10% of all freshwater in lakes on Earth, and the use of atmospheric water to solve the shortage of freshwater resources is attracting increased attention (Kim et al., 2017). First of all, scholars have used different methods to bionic the shape of cactus spines. Xu et al. (2016) prepared tapered copper wires with periodic roughness gradients through electrochemical etching. (Zhong et al., 2018) prepared one-dimensional double-gradient filaments by gradient electrochemical etching and gradient chemical modification. Heng et al. (2014) prepared a biomimetic cactus needle-like structure by vapor deposition.

TABLE 1 Detailed information of polyethylene terephthalate (PET).

	Wire diameter (mm)	Pore size (micron)
#50	0.15	359
#80	0.1	218
#120	0.07	142

Cao et al. (2014) fabricated cactus cone arrays by magnetic powder-assisted forming. To solve the static fog-harvesting problem, Peng et al. (2015) fabricated a magnetically responsive flexible conical array that can capture droplets by magnetic induction under no-wind conditions. (Tang et al., 2021) fabricated a wetting gradient tapered copper needle combining structural and chemical gradients, a small three-dimensional array device, and applied to fog collection. Although many experiments have used different materials and various methods, a flat structure with a better water-collection effect that can be mass produced through a simple method is needed. Bai et al. (2020) reported a cactus-inspired fog-harvesting method by simply changing 3D cones to 2D triangles. Wu et al. (2017) developed efficient anisotropic fog collection on mixed and oriented surfaces. Zhu et al. (2016) fabricated a super hydrophilic surface with two super hydrophobic circular patterns through a simple and fast route with excellent fog-collection performance. Hu et al. (2019) designed a hybrid membrane with asymmetric micro topology and anisotropic wettability that can achieve efficient fog collection. Zhang et al. (2021) fabricated a multi-level microstructure using treatments such as photolithography, acid etching, anodization, and fluoroalkyl silane modification, and successfully fabricated a surface with both good robustness and high efficiency water-harvesting properties. (Kong, 2021) formed dense and uniform nanoscale petal-like structures on the surface of phosphor copper meshes by a simple solution impregnation method. The surface exhibits excellent super hydrophobicity, facilitates the transport of various aqueous solutions without significant loss, and can be reused without additional cleaning. Wang et al. (2016) developed a fabric with a super hydrophobic surface incorporating light-induced super hydrophilic bumps.

To create treatment materials with the best water collection effect, many scholars have studied chemically modifying substrate materials to generate super hydrophilic/super hydrophobic surfaces. For example, Xu et al. (2017) successfully prepared a new type of surface through emulsion polymerization. Hydrophobically modified polymer-based silica nanocomposites; (Khedkar et al., 2019); Modification of silica gels by using trimethylchlorosilane (TMCS) as a silylating agent; (Björkegren et al., 2017); Hydrophobic functionalization of silica sols by linking organosilanes mainly containing propyl and methyl groups; (Wang et al., 2016); treated with OTES by a simple dip-pad-dry method to form a super hydrophobic fabric. Hashemizad et al. (2012) treated PET fabrics with an alkaline solution (sodium hydroxide), and topological chemical degradation resulted in surface PET chain scission through hydrolysis and introduction of hydrophilic groups such as OH and COOH on the fabric surface. Alkaline hydrolysis improves the hydrophilicity of PET fabrics, while increasing the fiber surface roughness and inter fiber/inter yarn capillary space; (Görgülüer et al., 2021); prepared super hydrophobic titanium dioxide (TiO_2)-polydimethylsiloxane (PDMS)-silver nanoparticles (Ag NPs) coatings on fabrics by a simple impregnation method. The layer exhibit super hydrophobicity; (Kutuzau et al., 2019); designed a «PET TM + TiO_2» modified TiO_2 PET film for photo catalytically active filtration system; (Cheng et al., 2017); Multilayer nanocomposite films with excellent UV protection were successfully prepared by depositing negatively and positively charged TiO_2 nanoparticles on PET films; (Xu and Li, 2021); Super hydrophobic TiO_2/SiO_2 nanoparticle-coated metal meshes, sponges, and loofahs were prepared by a simple spray method; (Zhou et al., 2006); TiO_2–SiO_2 thin films with high photocatalytic activity were prepared on modified PET substrates at low temperature by an advanced sol-gel method. After the PET substrate was modified with a silane coupling agent, the adhesion between the TiO_2-SiO_2 film and the substrate was improved.

Combining the above, hydrophobic modification of SiO_2, and PET deposition of TiO_2 yields a hydrophilic surface. In the study, in Figures 1,2, Hydrophilic and hydrophobic samples were obtained by dip coating and spray coating. On the base material PET, SiO_2 was first dip-coated, and then (octadecyltriethoxysilane) OTS was dip-coated to form a hydrophobic surface. The TiO_2 particles on a hydrophobic surface responded to UV light to obtain a hydrophilic surface (Gou and Guo, 2019). After 30 min of UV irradiation, WCA took a shorter time to change to 0° than before UV irradiation, indicating that the wettability of TiO_2 changed to hydrophilic (Wang et al., 2016). This hydrophilic condition can be maintained without light for at least 12 h, ensuring that good fog can capture the next night's storage and remain in the morning. The results of this research can provide a technique for addressing water shortages.

2 Materials and experiment

2.1 Materials

The base materials used were 50-, 80-, and 120-mesh PET. Detailed information is listed in Table 1. The PET materials were cut into small test pieces (3 cm × 3 cm). Sodium silicate solution (CP, SAMCHAUN), hydrochloric acid 35%–37% (SAMCHAUN), octadecyltriethoxysilane (98%), n-isomer (85% min; Alfa) (OTS), titanium isopropoxide (IV) (>98%; Acros), acetic acid (99.5%; SAMCHAUN), and ethanol were purchased from commercial sources.

2.2 Preparation of SiO_2 sol

First, 2 Mol HCl solution was prepared by diluting concentrated hydrochloric acid. Then, 5 g of sodium silicate solution was added to 50 ml of distilled water and stirred magnetically for 3–5 min at room temperature. Afterward, 2 Mol HCl solution was added dropwise to the stirred solution to adjust its pH to nine under magnetic stirring.

2.3 Preparation of TiO_2 sol

First, titanium (IV) isopropoxide (40 g) was added dropwise with a syringe to 100 ml of distilled water containing HAc (0.5wt %) and HCl (1wt%) with mechanical stirring at 350 rpm. Under magnetic stirring at 85°C, water was slowly added dropwise to the prepared mixture by using a syringe for 4 h, resulting in a milky white sol. This sol was then cooled to 60°C and magnetically stirred for 15 h until a transparent blue sol was obtained. The final TiO_2 sol was obtained after aging, and the obtained TiO_2 solid content was 10wt%.

2.4 Preparation of super hydrophobic meshes (dip coating)

First, the cut 50-, 80-, and 120-mesh PET (30 mm × 30 mm) samples were placed in an Analog Ultrasonic Cleaner (WUC-A, South Korea) to remove dust on the surface. For untreated substrate PET (P), it was denoted as mesh50P, mesh80P, or mesh120P according to wire diameter. Mesh50 P, mesh80 P, and mesh120 P were then immersed in SiO_2 sol for 1 min for dip coating. The filling was then carried out at a pressure of 2 kg/cm^2 to ensure even coverage of the SiO_2 particles. After drying in an oven at 40°C for 20 min, the obtained samples were hydrophilic SPs denoted as mesh50 SP, mesh80 SP, and mesh120 SP. The SPs were then dip-coated with 3wt% OTS with ethanol as a solvent for 30 min and dried at 40°C for 20 min. The obtained samples were OSPs with hydrophobicity denoted as mesh50 OSP, mesh80 OSP, and mesh120 OSP.

2.5 Preparation of super hydrophilic surfaces (spray coating)

A spray coater (SRC-100, E-flex) was used to spray TiO_2 sol onto the prepared hydrophobic OSP. At the same time, the heat treatment method is used, and the electroplating water is evaporated during the spraying process. The sprayed sample was then irradiated with UV light for 30 min to obtain mesh50 TOSP, mesh80 TOSP, and mesh120 TOSP. Different samples were prepared according to spraying distances varying from 5, 7, 9, 11, 13, and 15 cm.

2.6 Morphological research

Topographies of P, SP, OSP, and TOSP surfaces were observed using a field-emission scanning electron microscopy (FE-SEM) system (Desktop mini-SEM, SNE 3000 M, South Korea).

2.7 Energy dispersive X-ray

The TOSP elemental composition was analyzed using energy dispersive X-ray (UHR FE-SEM by Hitachi High-Technologies Corp., SU8230, Japan).

2.8 FT-IR

Infrared spectroscopy (FT-IR Spectrometer by Bruker, IFS66v/s, Hyperion3000, Alpha, Germany) was performed on P, SP, OSP, and TOSP.

2.9 Experimental setup for fog harvesting

The natural fog was simulated with an ultrasonic humidifier (SGH-U205R, South Korea). All prepared samples (bare P, SP, OSP, and TOSP with different spraying distances) were subjected to a 1 h water-catchment test. The mist flow was perpendicular to the sample. The collected water mass was measured and recorded with an electronic balance. A digital camera was used to photograph the water-catchment process. During the test, the temperature and humidity of the environment were also real-time measured. Make sure the experiments are performed at similar temperatures and humidity.

3 Results

3.1 Mimicking a cactus-stem catchment system

A hydrophilic–hydrophobic bilayer structure was developed by imitating the water-harvesting mechanism of the cactus. For the TOSP with a double-layer structure, the top layer TiO_2 particles were used to collect the fog. When nano-TiO_2 is irradiated with ultraviolet (UV) light, electrons are lifted from the valence band to the conduction band, causing the former to generate charged “holes”. (Fujishima et al., 2000; Chong et al., 2010). Free electrons react with oxygen to form superoxide radical anions (O^{2-}), while exciting holes react with water (H_2O) or hydroxide ions (OH^-) to form hydroxyl radicals (OH). Surface acidity, defects, and OH groups strongly influence the chemical

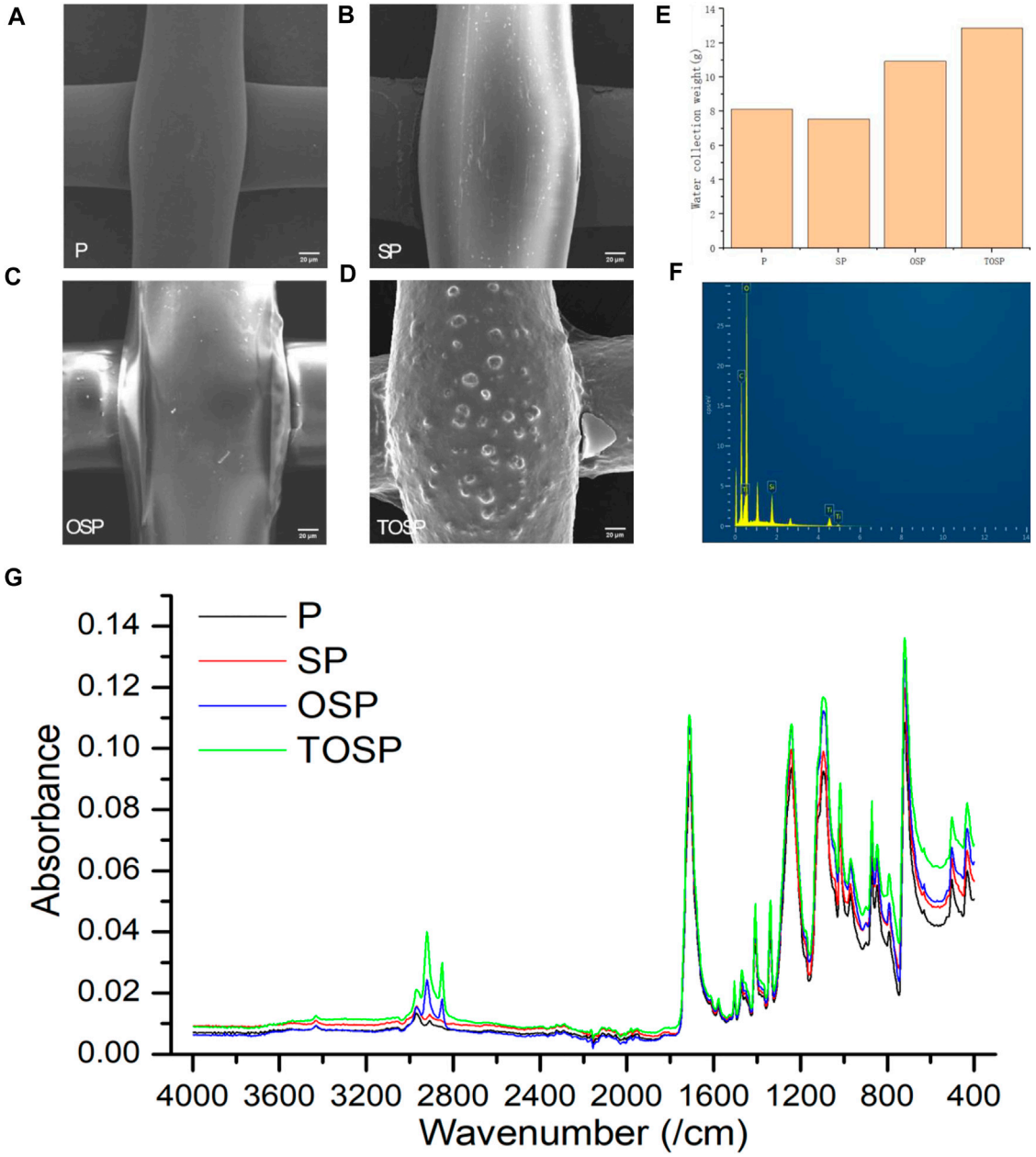

FIGURE 3
Taking mesh80 as an example, the field-emission scanning electron microscopy (FE-SEM) image of **(A)** untreated bare P (polyethylene terephthalate), **(B)** P dip coated with SiO_2 to obtain SP, **(C)** SP chemically modified by OTS to obtain OSP, **(D)** OSP sprayed with TiO_2 to obtain TOSP after the light response. **(E)** Histogram of catchment quality of P, SP, OSP, and TOSP. **(F)** Energy dispersive X-rays of TOSP. **(G)** Infrared spectroscopy was performed on P, SP, OSP, and TOSP.

properties of TiO_2 (Park and Choi, 2004). Surface acidification of TiO_2 has been reported to improve the adsorption and reaction of polar molecules. The photo-induced hydrophilicity was found to be due to structural changes on the surface of the material, completely different from conventional photocatalytic reactions. The key is the reconstruction of hydroxyl groups and their increased number on the sample surface under UV light irradiation. In detail, the photo generated holes are trapped by surface lattice oxygen atoms, resulting in the breaking of bonds between oxygen and titanium atoms. Subsequently, water molecules dissociative adsorb (form hydroxyl groups) at

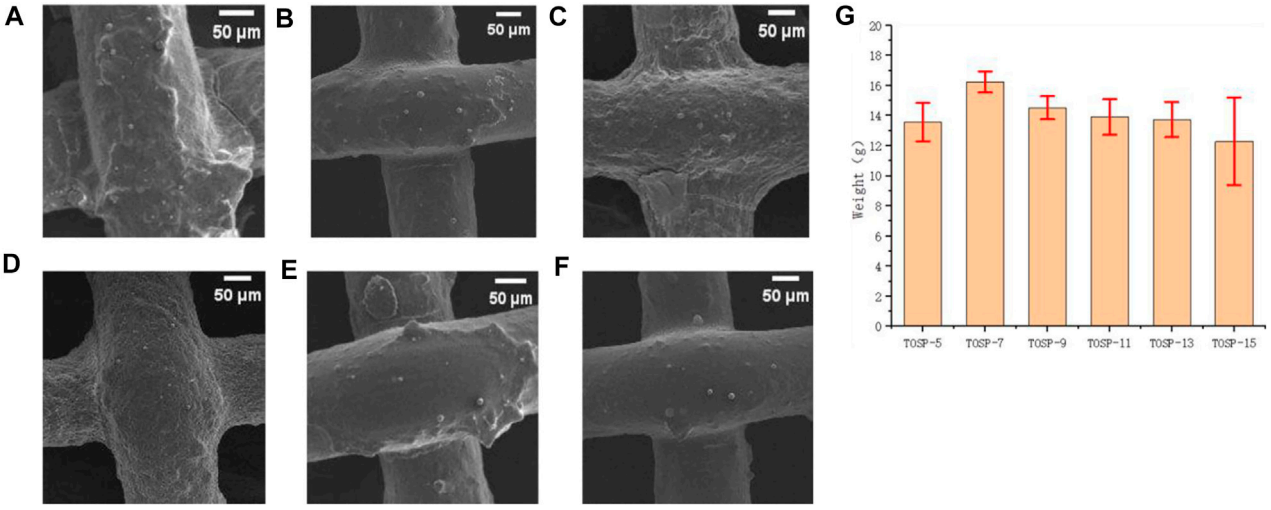

FIGURE 4
Field-emission scanning electron microscopy (FE-SEM) image of **(A)** mesh50 TOSP-5, **(B)** mesh50 TOSP-7, **(C)** mesh50 TOSP-9, **(D)** mesh50 TOSP-11, **(E)** mesh50 TOSP-13, **(F)** mesh50 TOSP-15, and **(G)** water collection histogram of mesh50 spraying distances of 5, 7, 9, 11, 13, and 15 cm.

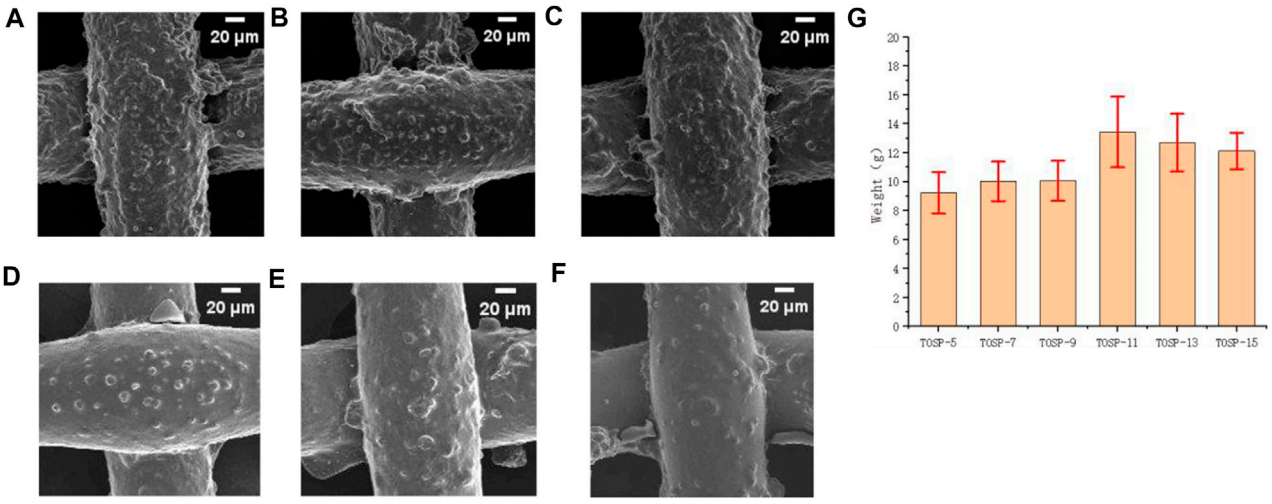

FIGURE 5
Field-emission scanning electron microscopy (FE-SEM) image of **(A)** mesh80 TOSP-5, **(B)** mesh80 TOSP-7, **(C)** mesh80 TOSP-9, **(D)** mesh80 TOSP-11, **(E)** mesh80 TOSP-13, **(F)** mesh80 TOSP-15, and (G) water collection histogram of mesh80 spraying distances of 5, 7, 9, 11, 13, and 15 cm.

these sites. Therefore, the bonding strength between oxygen and titanium is important for photo hydrophilicity. (Li et al., 2005; Wang, 2005; Gui, 2014; Wang et al., 2020). Due to the surface acidity, it is thought to be in the form of stronger surface hydroxyl groups. The stable hydroxyl groups on the surface are beneficial to maintain hydrophilicity, which may explain why the water contact angle of the composite membrane increases slowly and remains low for a long time in the dark (Guan et al., 2003). The principle of photo responsive TiO_2 is that the solid acid of the hydrogen bonding component that increases the surface energy of the solid/gas interface is supported on the surface of the photocatalytic coating. When the photo catalyst is excited by light, the hydrogen bonding

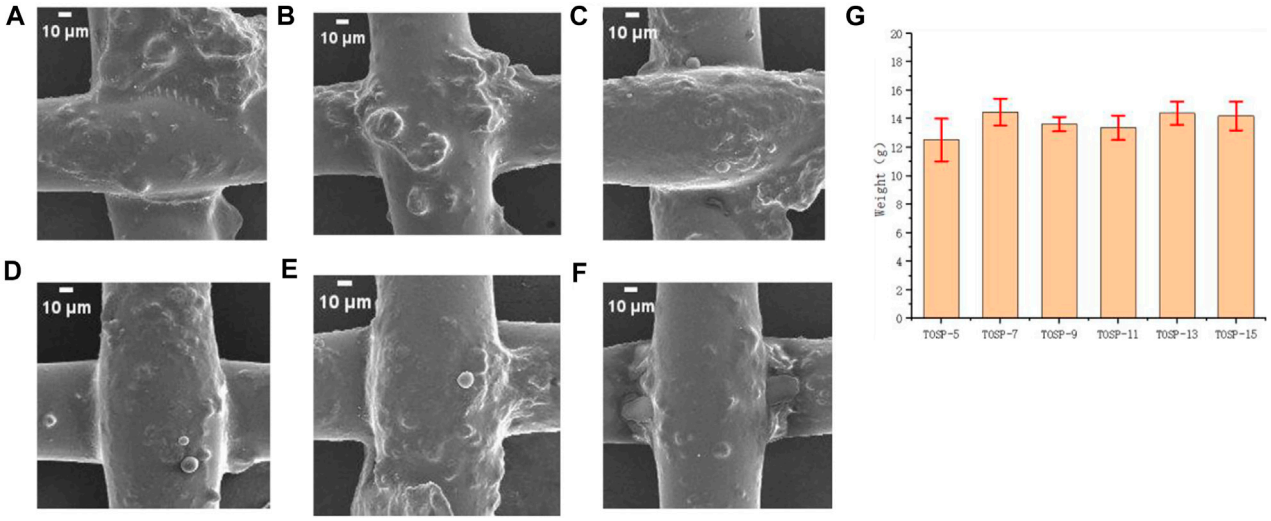

FIGURE 6
Field-emission scanning electron microscopy (FE-SEM) image of **(A)** mesh120 TOSP-5, **(B)** mesh120 TOSP-7, **(C)** mesh120 TOSP-9, **(D)** mesh120 TOSP-11, **(E)** mesh120 TOSP-13, **(F)** mesh120 TOSP-15, and **(G)** water collection histogram of mesh120 spraying distances of 5, 7, 9, 11, 13, and 15 cm.

component of the surface energy of the photo catalyst coating is increased by the photo catalyst, which promotes the physical adsorption of molecules. As a result, a high-density physically adsorbed water layer is formed on the surface of the photo catalyst coating, so that the surface is easily hydrophilized. The bottom layer was dip-coated with hydrophilic SiO_2 sol and then dip-coated with OTS to convert it into a hydrophobic sample to release the water droplets collected in the top layer.

3.2 Water-catchment analysis

Figures 3A–D shows the FE-SEM images of bare P, SP, OSP, and TOSP. After drying and filling with SiO_2 sol, the surface of polyester fiber was covered with a SiO_2 sol layer, which can increase the surface roughness. The average diameter of SiO_2 particles on the surface measured by ImageJ was 1.478 μm. Accordingly, the surface of polyester fiber became hydrophobic after OTS treatment with low surface energy. This hydrophobic polyester surface ensured the efficient release of water droplets. After the hydrophobic polyester was manufactured, the hydrophilic TiO_2 sol was introduced into the hydrophobic surface by spraying. TOSP with hydrophilic and hydrophobic bilayer structures were fabricated. The average diameter of TiO_2 particles on the surface measured by ImageJ was 6.271 μm. To study the efficiency of water collection, all samples were exposed to UV light (1.84 mW/cm^2) at 365 nm for 30 min (The same result can be obtained with 1 h of sunlight with a UV intensity of about 1 mW/cm^2) before water collection. The water collection was tested with a humidifier for naked P, SP, OSP, and all TOSP multiple times. After 1 h, the weight of each sample was recorded, and the water-collection results were compared. Figure 3E. Results showed that the TOSP sample had higher water-harvesting efficiency than bare P, SP, and OSP. In other words, the hydrophilic and hydrophobic bilayer structures TOSP had the more water-collection capacity and better water-collection effect than the hydrophilic SP and hydrophobic P and OSP. The presence of Si and Ti elements on TOSP can be observed in Figure 3F. In Figure 3G, 3,000–3,800 cm^{-1} belongs to the stretching mode of the O-H band, which is related to free water (capillary pore water and surface absorbed water) (Yu et al., 2001), in this range, the hydrophilic-hydrophobic TOSP is on top, followed by the hydrophilic SP, and the bottom is the overlapping OSP and P. The peak at about 1,600 cm^{-1} is due to the bending vibration of the H-O-H bond, which is assigned to chemisorbed water. In the sample, the 1,000–1,250 cm^{-1} band is clearly visible, which is attributed to the asymmetric stretching vibration of the Si-O-Si band. The absorption peaks at 775 and 470 cm^{-1} are attributed to the symmetrical stretching vibrations of the Si-O-Si band. The Si-O-Ti bond stretching band and the Si-OH band appear at about 935 cm^{-1}. (Pickup et al., 1999; Jung, 2000). The chemical modification of PET with SiO2, OTS, and TiO2 was well demonstrated.

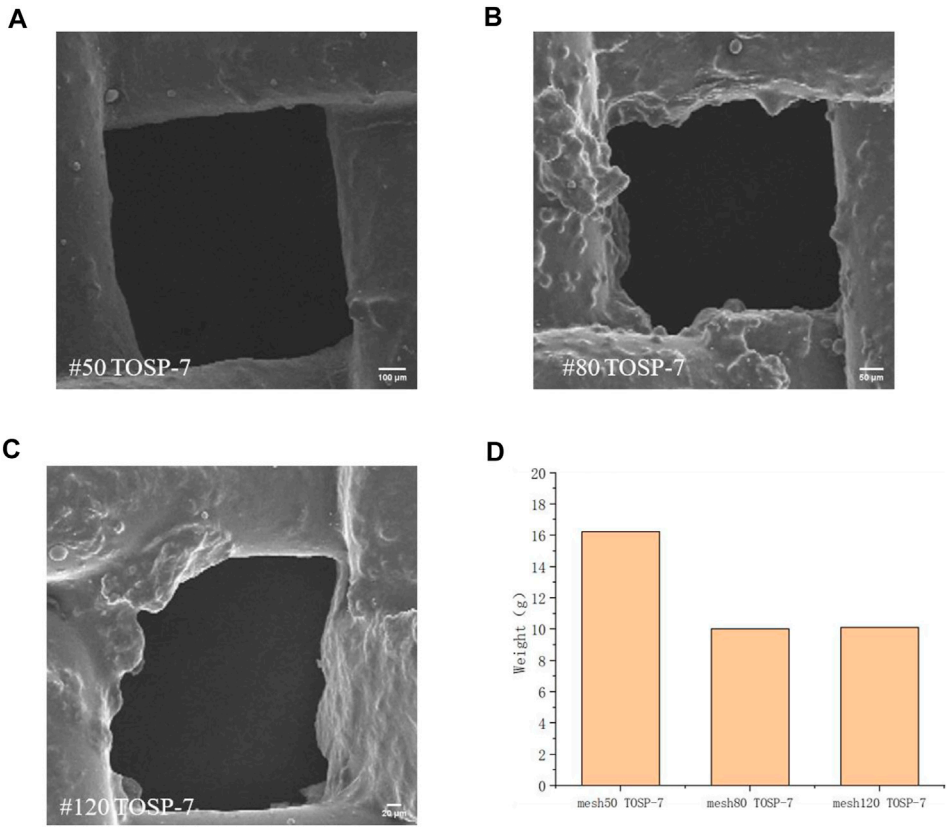

FIGURE 7
Field-emission scanning electron microscopy (FE-SEM) image of **(A)** mesh50 TOSP-7, **(B)** mesh80 TOSP-7, and **(C)** mesh120 TOSP-7. **(D)** Water-collection diagram of the three samples.

3.2.1 Effect of TiO_2 spraying distance

In mesh50, the distance between the spray-coating nozzle and the sample was 5, 7, 9, 11, 13, or 15 cm. Treated samples were subjected to UV irradiation for 30 min. At 25°C and about 60% humidity, all samples were subjected to a humidifier test for 1 h three times to determine the average value and the amount of moisture collected. Figures 4A–F FE-SEM image of mesh50 shows that a greater spraying distance meant a lower adhesion density of hydrophilic TiO_2 particles. The water-collection results revealed that the maximum water collection was that of TOSP-7, with a spraying distance of 7 cm. TOSP-7 had the most suitable particle-adhesion density of TiO_2, which can quickly capture fog and discharge water immediately. When the spraying distance was less than 7 cm, the particle-adhesion density of TiO_2 was high, so the fog capture efficiency was high. However, considering that the hydrophilic TiO_2 particles covered the hydrophobic layer OSP to a certain extent, water was difficult to discharge immediately, so the water-collection amount was small. When the spraying distance was greater than 7 cm, the particle-adhesion density of TiO_2 was low and the fog capture efficiency was low, so the water collection was small. Figure 4G TOSP-7: 16.23 g.

Under the same conditions, in mesh80, Figures 5A–F FE-SEM image of mesh80 showed that a greater spraying distance corresponded with a lower adhesion density of hydrophilic TiO_2 particles. The water-collection results showed that the maximum water collection was that of TOSP-11, with a spraying distance of 11 cm. TOSP-11 had the most suitable particle-adhesion density of TiO_2, which can quickly capture fog and immediately discharge water. When the spraying distance was less than 11 cm, the particle-adhesion density of TiO_2 was high, so the fog capture efficiency was high. However, because the hydrophilic TiO_2 particles overlapped with one another and covered the hydrophobic layer OSP, discharging the water was difficult, so the water collection was small. For TOSP with a spraying distance greater than 11 cm, the particle-adhesion density of TiO_2 and the fog-capture efficiency were low, so the water collection was small. Figure 5G TOSP-11: 13.44 g.

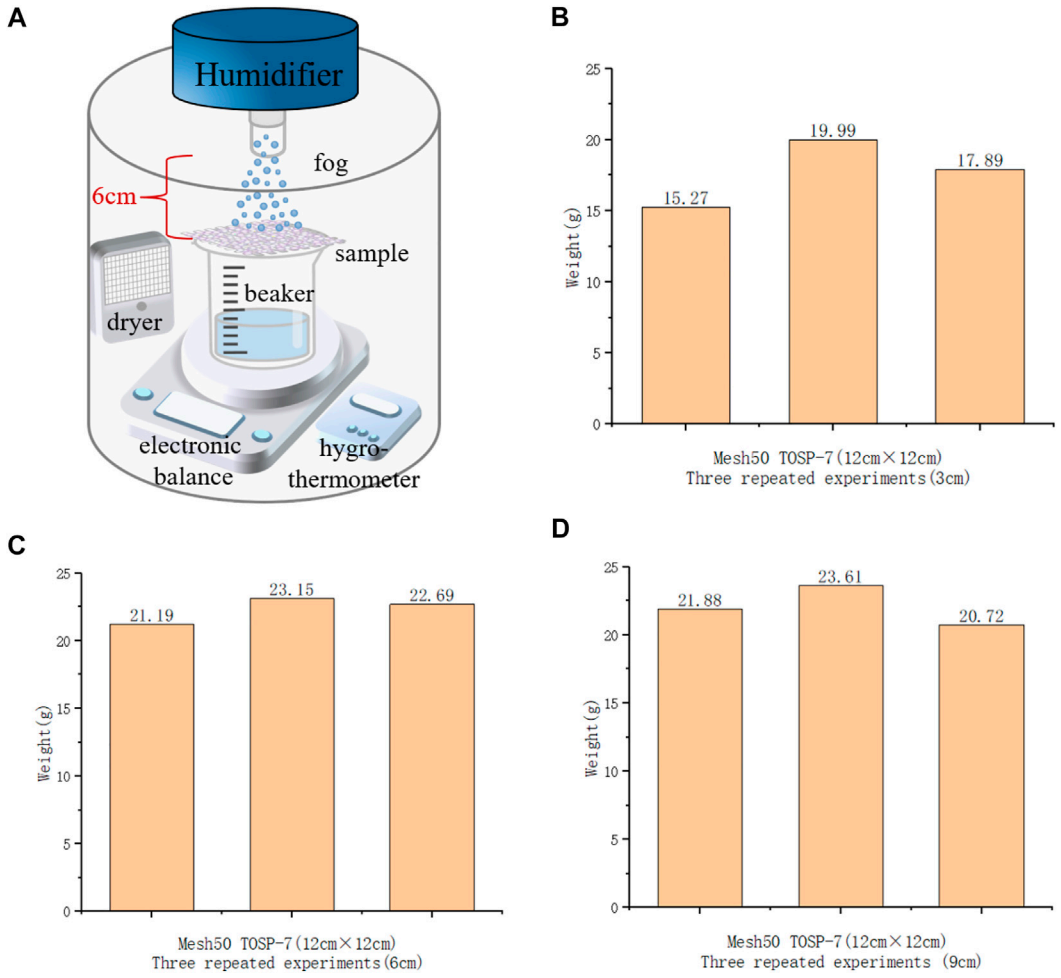

FIGURE 8
Self-made device for testing the water-collection capacity of the sample and the results of the three tests. **(A)** The water-collection test was conducted in a relatively sealed and transparent acrylic box, subject to as little influence of external humidity and temperature as possible. The humidifier sprays simulated atmospheric fog and sprayed the sample on the beaker. The mist made contact with the hydrophilic area of the sample and was absorbed, and the water droplets gradually enlarged, touching the hydrophobic area of the sample. The water droplets were discharged into the beaker. The electronic balance display shows the amount of water collected, and the camera can record the real-time change in the balance display. **(B)** Histogram of three times water collection after sample expansion (the original sample was 3 cm × 3 cm, but owing to the limitation of the size of the loading platform of the spraying equipment and ultrasonic scrubber, the sample was enlarged to 12 cm × 12 cm). The distances between the nozzle of the humidifier and the sample of 3 cm, **(C)** 6 cm, and **(D)** 9 cm.

Under the same conditions, in mesh120 with the same wire diameter, Figures 6A–F given that the wire diameter and pore diameter of mesh120 were very small, the hydrophilic TiO_2 particles overlapped with one another and covered the hydrophobic layer OSP. The absorbed water droplets cannot quickly touch the hydrophobic layer, and the water-discharge time became longer, so the water-collection amount was small. Moreover, the size of the treated hole was smaller than that of water droplets, and the water droplets were stuck in the hole diameter for a long time. Only when the water droplets gathered to a certain extent did they fall owing to gravity, so the water collection was small. For mesh 120, the spraying distance had little effect on the water collection. Figure 6G TOSP-7: 14.46 g.

3.2.2 Effect of different meshes

In Figure 7 with the same spraying distance of 7 cm, mesh 50 can quickly capture fog and discharge water, thereby balancing fog capture and water discharge well. Consequently, the water collection was the highest. For mesh80, because the hydrophilic TiO_2 particles after spraying photoreaction overlapped with one another and the hydrophobic layer OSP was covered to a certain extent, the water-discharge efficiency was low and the water

collection was small; For mesh120, because the hydrophilic TiO_2 particles after spraying photoreaction overlapped with one another, the hydrophobic layer OSP was covered, and the hole was also reduced to a certain extent. Thus, the water-discharge efficiency was low and the water collection was small.

3.3 Sample expansion experiments

To ensure that the final material processed by the experiment could be used in real life, the sample was expanded for the experiment. Mesh50 TOSP-7 with the highest water-collection rate in the above experiments was selected. Considering the size of the existing ultrasonic scrubber and the stage of the spraying equipment, the original mesh50 substrate PET (P) 3 cm × 3 cm sample was enlarged only to 12 cm × 12 cm. Then, the same treatment conditions as TOSP-7 were used. As shown in Figure 8A, the resulting final sample was subjected to a humidifier test to detect the water-collection rate of the expanded sample. In Figures 8B–D, after experiments were carried out on the distances between the nozzle of the humidifier and the sample of 3, 6, and 9 cm, the maximum average water collection amount was 22.34 g when the distance was 6 cm.

4 Discussion

TOSP with hydrophilic and hydrophobic bilayer structures were obtained by simple dip coating and spray coating methods. UV exposure can also be changed to longer sunlight exposure, and since sunlight is a sustainable energy source, super hydrophilic triggering of TiO_2 can be achieved without additional effort. Then, the effects of different wire diameters and different spraying distances on the quality of collected moisture were studied. When the PET is mesh50 and the spraying distance is 7 cm, the water collection effect is the best. In order to apply this technology to real life, the original mesh50 TOS-7 sample was expanded and subjected to the same processing and testing. Overall, this study provides a method to further improve the hydrophilicity and hydrophobicity of samples, which can be used in foggy and water-deficient regions.

Data availability statement

The original contributions presented in the study are included in the article/Supplementary Material, further inquiries can be directed to the corresponding author.

Author contributions

KK and YS contributed to the conception and design of the study. YS conducted the experiments, organized the database, performed the statistical analysis, and wrote the first draft of the manuscript. All authors participated in the revision of the manuscript, read and approved the submitted version.

Funding

This work was supported by the National Research Foundation of Korea (NRF) grant funded by the Korea government (MSIT) (No. NRF-2020R1C1C1003813).

Conflict of interest

The authors declare that the research was conducted in the absence of any commercial or financial relationships that could be construed as a potential conflict of interest.

Publisher's note

All claims expressed in this article are solely those of the authors and do not necessarily represent those of their affiliated organizations, or those of the publisher, the editors and the reviewers. Any product that may be evaluated in this article, or claim that may be made by its manufacturer, is not guaranteed or endorsed by the publisher.

References

Bai, H., Zhao, T., Wang, X., Wu, Y., Li, K., Yu, C., et al. (2020). Cactus kirigami for efficient fog harvesting: Simplifying a 3D cactus into 2D paper art. *J. Mat. Chem. A* 8 (27), 13452–13458. doi:10.1039/D0TA01204A

Björkegren, S., Nordstierna, L., Törncrona, A., and Palmqvist, A. (2017). Hydrophilic and hydrophobic modifications of colloidal silica particles for Pickering emulsions. *J. Colloid Interface Sci.* 487, 250–257. doi:10.1016/j.jcis.2016.10.031

Cao, M., Ju, J., Li, K., Dou, S., Liu, K., and Jiang, L. (2014). Facile and large-scale fabrication of a cactus-inspired continuous fog collector. *Adv. Funct. Mat.* 24 (21), 3235–3240. doi:10.1002/adfm.201303661

Cheng, D., Cai, G., Wu, J., Ran, J., and Wang, X. (2017). UV protective PET nanocomposites by a layer-by-layer deposition of TiO2 nanoparticles. *Colloid Polym. Sci.* 295 (11), 2163–2172. doi:10.1007/s00396-017-4178-6

Chong, M. N., Jin, B., Chow, C. W., and Saint, C. (2010). Recent developments in photocatalytic water treatment technology: A review. *Water Res.* 44 (10), 2997–3027. doi:10.1016/j.watres.2010.02.039

Fujishima, A., Rao, T. N., and Tryk, D. A. (2000). Titanium dioxide photocatalysis. *J. Photochem. Photobiol. C Photochem. Rev.* 1 (1), 1–21. doi:10.1016/S1389-5567(00)00002-2

Görgülüer, H., Çakıroğlu, B., and Özacar, M. (2021). Ag NPs deposited TiO2 coating material for superhydrophobic, antimicrobial and self-cleaning surface fabrication on fabric. *J. Coat. Technol. Res.* 18 (2), 569–579. doi:10.1007/s11998-020-00412-6

Gou, X., and Guo, Z. (2019). Hybrid hydrophilic–hydrophobic CuO@ TiO2-coated copper mesh for efficient water harvesting. *Langmuir* 36 (1), 64–73. doi:10.1021/acs.langmuir.9b03224

Guan, K., Lu, B., and Yin, Y. (2003). Enhanced effect and mechanism of SiO2 addition in super-hydrophilic property of TiO2 films. *Surf. Coat. Technol.* 173 (2-3), 219–223. doi:10.1016/S0257-8972(03)00521-8

Gui, Y. (2014). Influences of titanium oxide additions on the electrochromic properties of WO3 thin films. Available at: http://scholarbank.nus.edu.sg/handle/10635/119280, (Accessed 10 March 2015)

Hashemizad, S., Montazer, M., and Rashidi, A. (2012). Influence of the surface hydrolysis on the functionality of poly (ethylene terephthalate) fabric treated with nanotitanium dioxide. *J. Appl. Polym. Sci.* 125 (2), 1176–1184. doi:10.1002/app.35381

Heng, X., Xiang, M., Lu, Z., and Luo, C. (2014). Branched ZnO wire structures for water collection inspired by cacti. *ACS Appl. Mat. Interfaces* 6 (11), 8032–8041. doi:10.1021/am4053267

Hu, R., Wang, N., Hou, L., Cui, Z., Liu, J., Li, D., et al. (2019). A bioinspired hybrid membrane with wettability and topology anisotropy for highly efficient fog collection. *J. Mat. Chem. A* 7 (1), 124–132. doi:10.1039/c8ta10615k

Ju, J., Bai, H., Zheng, Y., Zhao, T., Fang, R., and Jiang, L. (2012). A multi-structural and multi-functional integrated fog collection system in cactus. *Nat. Commun.* 3 (1), 1–6. doi:10.1038/ncomms2253

Jung, M. (2000). Synthesis and structural analysis of Au-doped TiO2/SiO2 mixed oxide films prepared by sol-gel process. *J. Solgel. Sci. Technol.* 19 (1), 563–568. doi:10.1023/A:1008748924836

Khedkar, M. V., Somvanshi, S. B., Humbe, A. V., and Jadhav, K. (2019). Surface modified sodium silicate based superhydrophobic silica aerogels prepared via ambient pressure drying process. *J. Non. Cryst. Solids* 511, 140–146. doi:10.1016/j.jnoncrysol.2019.02.004

Kim, H., Yang, S., Rao, S. R., Narayanan, S., Kapustin, E. A., Furukawa, H., et al. (2017). Water harvesting from air with metal-organic frameworks powered by natural sunlight. *Science* 356 (6336), 430–434. doi:10.1126/science.aam8743

Kong, L.-H. (2021). An environmentally friendly method for fabrication of superhydrophobic "pipe" with loss-free liquid transportation properties. *Surf. Coat. Technol.* 407, 126777. doi:10.1016/j.surfcoat.2020.126777

Kutuzau, M., Shumskaya, A., Kaniukov, E., Alisienok, O., Shidlouskaya, V., Melnikova, G., et al. (2019). Photocatalytically active filtration systems based on modified with titanium dioxide PET-membranes. *Nucl. Instrum. Methods Phys. Res. Sect. B Beam Interact. Mater. Atoms* 460, 212–215. doi:10.1016/j.nimb.2019.01.028

Lee, S. J., Ha, N., and Kim, H. (2019). Superhydrophilic–superhydrophobic water harvester inspired by wetting property of cactus stem. *ACS Sustain. Chem. Eng.* 7 (12), 10561–10569. doi:10.1021/acssuschemeng.9b01113

Li, D., Haneda, H., Hishita, S., Ohashi, N., and Labhsetwar, N. K. (2005). Fluorine-doped TiO2 powders prepared by spray pyrolysis and their improved photocatalytic activity for decomposition of gas-phase acetaldehyde. *J. Fluor. Chem.* 126 (1), 69–77. doi:10.1016/j.jfluchem.2004.10.044

Liu, M., Wang, S., and Jiang, L. (2017). Nature-inspired superwettability systems. *Nat. Rev. Mat.* 2 (7), 1–17. doi:10.1038/natrevmats.2017.36

Mekonnen, M. M., and Hoekstra, A. Y. (2016). Four billion people facing severe water scarcity. *Sci. Adv.* 2 (2), e1500323. doi:10.1126/sciadv.1500323

Park, H., and Choi, W. (2004). Effects of TiO2 surface fluorination on photocatalytic reactions and photoelectrochemical behaviors. *J. Phys. Chem. B* 108 (13), 4086–4093. doi:10.1021/jp036735i

Parker, A. R., and Lawrence, C. R. (2001). Water capture by a desert beetle. *Nature* 414 (6859), 33–34. doi:10.1038/35102108

Peng, Y., He, Y., Yang, S., Ben, S., Cao, M., Li, K., et al. (2015). Magnetically induced fog harvesting via flexible conical arrays. *Adv. Funct. Mat.* 25 (37), 5967–5971. doi:10.1002/adfm.201502745

Pickup, D., Mountjoy, G., Wallidge, G., Anderson, R., Cole, J., Newport, R, J., et al. (1999). A structural study of (TiO2)x(SiO2)1−x (x=0.18, 0.30 and 0.41) xerogels prepared using acetylacetone. *J. Mat. Chem.* 9, 1299–1305. doi:10.1039/A809810G

Postel, S. L., Daily, G. C., and Ehrlich, P. R. (1996). Human appropriation of renewable fresh water. *Science* 271 (5250), 785–788. doi:10.1126/science.271.5250.785

Tang, X., Huang, J., Guo, Z., and Liu, W. (2021). A combined structural and wettability gradient surface for directional droplet transport and efficient fog collection. *J. Colloid Interface Sci.* 604, 526–536. doi:10.1016/j.jcis.2021.07.033

Van Der Vegt, G. S., Essens, P., Wahlström, M., and George, G. (2015). *Managing risk and resilience*. NY: Academy of Management Briarcliff Manor.

Vorosmarty, C. J., Green, P., Salisbury, J., and Lammers, R. B. (2000). Global water resources: Vulnerability from climate change and population growth. *Science* 289 (5477), 284–288. doi:10.1126/science.289.5477.284

Wang, T., Jiang, L.-l., Huang, L.-l., Wu, L.-g., Li, C.-j., and Cai, J. (2020). Photo-induced antifouling polyvinylidene fluoride ultrafiltration membrane driven by weak visible light. *J. Ind. Eng. Chem.* 89, 476–484. doi:10.1016/j.jiec.2020.06.027

Wang, X. (2005). *Functionalized porous titania nanostructures as efficient photocatalysts*. Hong Kong: The Chinese University of Hong Kong.

Wang, Y., Wang, X., Lai, C., Hu, H., Kong, Y., Fei, B., et al. (2016). Biomimetic water-collecting fabric with light-induced superhydrophilic bumps. *ACS Appl. Mat. Interfaces* 8 (5), 2950–2960. doi:10.1021/acsami.5b08941

Wu, J., Zhang, L., Wang, Y., and Wang, P. (2017). Efficient and anisotropic fog harvesting on a hybrid and directional surface. *Adv. Mat. Interfaces* 4 (2), 1600801. doi:10.1002/admi.201600801

Xu, J.-g., Qiu, Z., Zhao, X., and Huang, W. (2017). Hydrophobic modified polymer based silica nanocomposite for improving shale stability in water-based drilling fluids. *J. Pet. Sci. Eng.* 153, 325–330. doi:10.1016/j.petrol.2017.04.013

Xu, P., and Li, X. (2021). Fabrication of TiO2/SiO2 superhydrophobic coating for efficient oil/water separation. *J. Environ. Chem. Eng.* 9 (4), 105538. doi:10.1016/j.jece.2021.105538

Xu, T., Lin, Y., Zhang, M., Shi, W., and Zheng, Y. (2016). High-efficiency fog collector: Water unidirectional transport on heterogeneous rough conical wires. *ACS Nano* 10 (12), 10681–10688. doi:10.1021/acsnano.6b05595

Xue, Z.-x., and Jiang, L. (2012). Bioinspired underwater superoleophobic surfaces. *Acta Polym. Sin.* 10, 1091–1101. doi:10.3724/SP.J.1105.2012.12101

Yu, J., Zhao, X., Yu, J. C., Zhong, G., Han, J., and Zhao, Q. (2001). The grain size and surface hydroxyl content of super-hydrophilic TiO2/SiO2 composite nanometer thin films. *J. Mat. Sci. Lett.* 20 (18), 1745–1748. doi:10.1023/A:1012458411717

Zhang, Y., Wang, T., Wu, M., and Wei, W. (2021). Durable superhydrophobic surface with hierarchical microstructures for efficient water collection. *Surf. Coat. Technol.* 419, 127279. doi:10.1016/j.surfcoat.2021.127279

Zheng, Y., Bai, H., Huang, Z., Tian, X., Nie, F.-Q., Zhao, Y., et al. (2010). Directional water collection on wetted spider silk. *Nature* 463 (7281), 640–643. doi:10.1038/nature08729

Zhong, L., Zhang, R., Li, J., Guo, Z., and Zeng, H. (2018). Efficient fog harvesting based on 1D copper wire inspired by the plant pitaya. *Langmuir* 34 (50), 15259–15267. doi:10.1021/acs.langmuir.8b03418

Zhou, L., Yan, S., Tian, B., Zhang, J., and Anpo, M. (2006). Preparation of TiO2–SiO2 film with high photocatalytic activity on PET substrate. *Mat. Lett.* 60 (3), 396–399. doi:10.1016/j.matlet.2005.08.065

Zhu, H., Yang, F., Li, J., and Guo, Z. (2016). High-efficiency water collection on biomimetic material with superwettable patterns. *Chem. Commun.* 52 (84), 12415–12417. doi:10.1039/C6CC05857D